



Heating rate modulates the metabolic response of the staghorn coral *Acropora cervicornis* (Lamarck, 1816)

Harmony A. Martell^{1,3} · Richard C. Zimmerman²

Received: 14 May 2020 / Accepted: 17 February 2021 / Published online: 8 May 2021
© The Author(s), under exclusive licence to Springer-Verlag GmbH, DE part of Springer Nature 2021

Abstract

Corals are relatively stenothermic organisms and highly sensitive to thermal stress. To understand how heating rate modulates the holobiont response to thermal challenge, we compared the effects of acute heat shock and cumulative thermal exposures on *Acropora cervicornis* from Southeast Florida (26° 06 N, 80° 05 W). In March of 2017, maximum dark-adapted yield of photosystem II (F_V/F_M), rates of dark respiration (R), and rates of gross photosynthesis (P_g) were measured at temperatures spanning 25–36 °C. Thermal performance curves of each response variable were constructed as a function of temperature and thermal dose (i.e., degree heating minutes). Acute exposure (i.e., instantaneously increasing temperature by between 2.5 and 10 °C) resulted in a more marked decline in physiology despite a lower thermal dose, compared to the cumulative exposure (2.5 °C h⁻¹). Apparent deficits in coral holobiont metabolism were observed as a function of both temperature and thermal dose, but examination of holobiont metabolism in a dose-context revealed more pronounced differences between acute and cumulative exposures. Subtle physiological differences may be more easily identified and better cross-study comparisons of cnidarian thermal tolerance may be achieved by placing temperature exposures in degree heating times. In addition, the ratio of daily $P_g:R$ fell below 1 when temperatures exceeded 32 °C, corroborating prior observations that $P_g:R$ may be a means of identifying physiological deficits in advance of visual signs of dysbiosis, such as bleaching.

Introduction

Corals participate in an intricate partnership with endosymbiotic dinoflagellates in the family Symbiodiniaceae (LaJeunesse et al. 2018) that provide most of the metabolic energy for survival (Muscatine et al. 1981) and growth (Muscatine and Cernichiari 1969). Under optimal conditions of light and temperature, corals provide their symbiotic partners with the carbon dioxide (CO₂) required for photosynthesis and the nutrients required for growth (Davy et al. 2012). In

exchange, the Symbiodiniaceae provide the host with photosynthetically fixed carbon in the forms of glucose (Burriesci et al. 2012), glycerol (Grottoli et al. 2006), lipids (Chen et al. 2015), and carbon skeletons for the synthesis of amino acids (Wang and Douglas 1999) and organo-phosphates (Morris et al. 2019). This exchange contributes to high productivity and enhanced calcification that enables reef formation in otherwise oligotrophic waters (Roth 2014).

Scleractinian corals are living near the upper limit of their thermal tolerance and are often especially sensitive to deviations > 1 °C above local temperature maxima, particularly in concert with sustained, high levels of irradiance (Fitt and Warner 1995; Lesser and Farrell 2004; Hoegh-Guldberg et al. 2017). Thermal and/or irradiance stress results in dysbiosis—the maladaptive perturbation of the normal coral-associated microbiome (Bosch and Miller 2016). Dysbiosis often involves the loss of endosymbiont chlorophyll or the Symbiodiniaceae via subsequent expulsion, digestion, and/or *in hospite* degradation that manifests visually as coral bleaching (Brown 1997; Lesser 2006; Weis 2008). Consequently, coral bleaching represents the biggest threat to the persistence of coral reef ecosystems worldwide (Hughes et al. 2003; Hoegh-Guldberg et al. 2017).

Responsible Editor: D. Gochfeld.

Reviewers: undisclosed experts.

✉ Harmony A. Martell
harmony.martell@ubc.ca

¹ Department of Biological Sciences, Old Dominion University, Norfolk, VA 23529, USA

² Department of Ocean and Earth Sciences, Old Dominion University, Norfolk, VA 23529, USA

³ Present Address: Department of Geography, The University of British Columbia, 1984 West Mall, Vancouver, BC V6T 1Z2, Canada

Measures of maximum dark-adapted yield of photosystem II (F_V/F_M), gross photosynthesis (P_g), and dark respiration (R) provide an integrated physiological perspective for interpreting the effects of temperature on cnidarian symbiosis (Coles and Jokiel 1977; Falkowski 1984; Davies 1991; Gates et al. 1992; Warner et al. 1999). Hundreds of studies have compared the physiological effects of heat-shocked cnidarians to control organisms held at ambient temperatures (reviewed in McLachlan et al. 2020). However, differences in heating rates and exposure regimes, even among short-term thermal stress experiments, make it difficult to resolve differences in results across studies (McLachlan et al. 2020). Indices of thermal accumulation, such as degree heating weeks, are used in products to warn managers about bleaching risks (Liu et al. 2018) and provide more accurate predictions of coral bleaching than temperature alone (Gleeson and Strong 1995). In these indices, degree heating times accumulate whenever temperatures exceed local mean monthly maxima (Wyatt et al. 2020). The same principle can be applied to laboratory temperature series to estimate thermal doses, since thermal stress and bleaching depend on dose and heating rate (Middlebrook et al. 2010). The majority of studies have examined coral performance as a function of temperature rather than thermal dose (McLachlan et al. 2020), but an improved understanding of coral bleaching and resilience could be achieved by examining coral performance in a dose-context.

We compared the metabolic responses (i.e., the activation energy, E_a , inactivation energy, E_h , and the temperature of inactivation, T_h , of F_V/F_M , R , and P_g) of *Acropora cervicornis* to determine how acute and cumulative heating regimes influence coral physiology. We hypothesized differences in coral physiology between acute and cumulative exposure would be more pronounced when related to thermal dose, rather than as a function of temperature. Responses are presented as a function of both temperature and degree heating minutes to demonstrate the value of each approach.

Materials and methods

Coral sampling

Nubbins of the staghorn coral *A. cervicornis* Lamarck were obtained from a nearshore coral nursery in Broward County, Florida (26° 06' N, 80° 05' W) maintained by Nova Southeastern University (NSU). *A. cervicornis* was chosen because it is one of two ecologically important acroporids that historically dominated the Caribbean reefscape, and it is a target species in a large number of restoration efforts (Schopmeyer et al. 2017). The source colonies used in this study were maintained in the nursery for > 6 years (5–7 m

depth, temperature series in Fig. 1a, inset). A total of seven genets of local origin were collected from the nursery to incorporate natural biological variability in the experimental design and broaden the applicability of our findings. The genets were previously identified by DNA microsatellite loci sequencing (Baums et al. 2010; Baums, unpublished data), and designated B through J. Genets were selected a priori by the nursery manager to represent a wide range of coral resilience based on outplant survival (Goergen and Gilliam 2018). In late February 2017, six 4-cm ramets from six genets (B, C, E, F, H, J), plus a single ramet from an additional genet (D), were cut from nursery colonies with bone cutters by SCUBA divers. The additional genet D nubbin was included to increase sample size. Each nubbin was glued to a hex-head bolt in situ with marine epoxy, tagged, and attached to a grid on a PVC array 0.5 m above the sandy seafloor. The resulting nubbins ($n = 6 \text{ genets} \times 6 \text{ ramets} = 36 + 1 = 37$ nubbins) were left to heal for 1 month. A HOBO logger (Onset Corp.) was attached to the array to record in situ temperature every 30 s (Fig. 1a, in situ nursery).

After one month, 36 of the selected nubbins had healed completely and grown. Only one nubbin died (genet F). The surviving nubbins were collected from the field nursery (in situ temperature at collection = 23.8 °C) and transported to the laboratory in an insulated cooler filled with seawater. Nubbins were placed in a common outdoor tank (1.5 m³ volume) with multi-directional, circulating seawater, and temperature control in NSU's land-based nursery. As in the field, temperature was recorded every 30 s by a HOBO logger (temperature range = 24.5–26.0 °C, Fig. 1a, tank). Encrusting organisms were gently removed with a handheld rotary tool from areas without live tissue. All nubbins were rinsed and returned to the outdoor tank for 2–5 days.

Irradiances

Estimates of maximum instantaneous downwelling irradiance at midday (E_{d_noon}) were calculated to approximate in situ light conditions at the nursery. Values of daily integrated photosynthetically available radiation (PAR) reaching the ocean surface and the diffuse attenuation coefficient, $K_d(490)$, were obtained for the location of the coral nursery during the month of March 2017 from the NASA MODIS program (<https://modis.gsfc.nasa.gov/data/dataproduct/par.php>) and inverted to produce instantaneous downwelling plane irradiances at noon [$E_{d_noon}(0+)$] incident on the surface, assuming a sinusoidal daily temporal pattern of irradiance:

$$\text{MODIS Daily PAR} = E_{d_noon}(0+) \int_{t=0}^{t=D} \sin\left(\pi \frac{t}{D}\right) dt$$

where $E_{d_noon}(0+)$ represents the instantaneous plane irradiance (PAR) above water at noon, t represents the time of day,

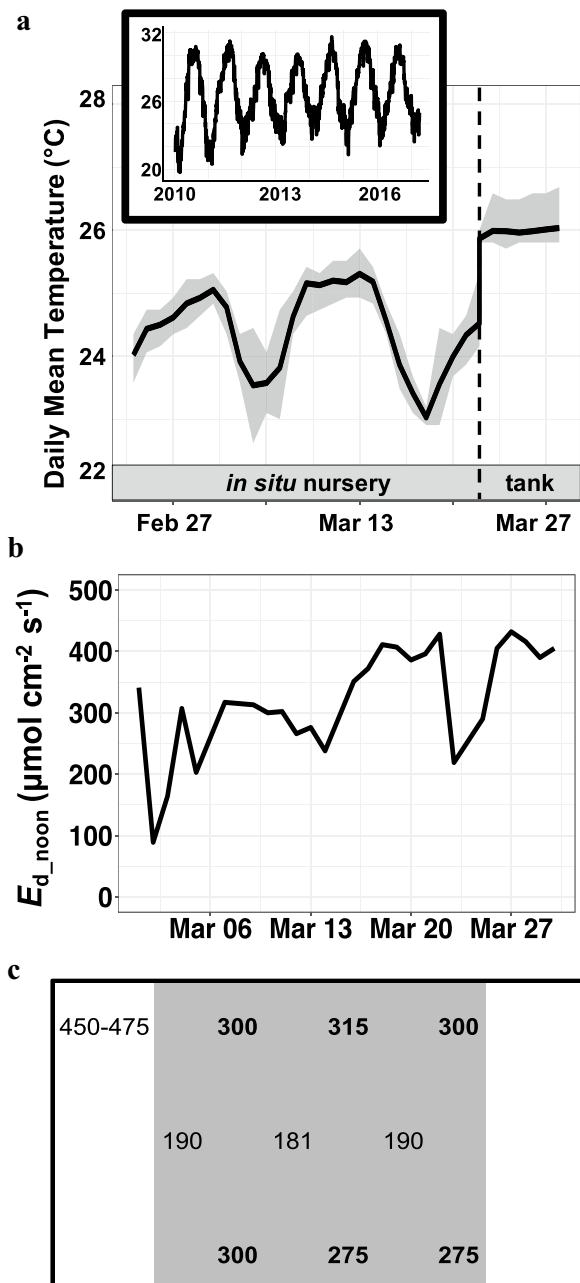


Fig. 1 Temperature series of **a** in situ nursery temperatures from the day corals were fragmented (February 22, 2017) until the day of collection (March 22, 2017, dashed line) and the outdoor common tank from the collection date until the last experimental day (March 27, 2017). Daily mean temperature (solid line) and daily range (shading) are displayed. Historical in situ field temperatures in the nursery from January 2010 to March 2017 (inset). **b** MODIS-derived daily noon irradiance (E_{d_noon}) for the field nursery ($z=6.1$ m) in March 2017. **c** A diagram of the outdoor tank with PAR measurements taken at mid-day (12:16). PAR values were taken at in each position in the tank, with bold numbers representing positions where corals were placed. The grey area represents the portion of the tank covered by a shade cloth

and D represents the daylength. The indefinite integral $\int \sin\left(\pi \frac{t}{D}\right) dt$ evaluates to $-\frac{1}{\pi} \cos\left(\pi \frac{t}{D}\right)$, which simplifies to $\frac{2D}{\pi}$ over the interval between sunrise ($t=0$) and sunset ($t=D$). This was rearranged to solve for $E_{d_noon}(0+)$:

$$E_{d_noon}(0+) = \frac{\pi \text{ MODIS Daily PAR}}{2D}$$

which was then propagated across the air–water interface using a transmittance (τ) of 0.54 (Mobley 1994) to obtain the in-water downwelling irradiance at the ocean surface:

$$E_{d_noon}(0-) = \tau E_{d_noon}(0+)$$

Instantaneous noon irradiances at the depth of the coral nursery, $E_{d_noon}(z)$, were then calculated using the Beer–Lambert Law:

$$E_{d_noon}(z) = E_{d_noon}(0-) \exp[-K_d(\text{PAR})z]$$

where z is the depth of the coral nursery (6.1 m) and $K_d(\text{PAR})$ was derived from MODIS $K_d(490)$ data product according to Morel et al. (2007):

$$K_d(\text{PAR}) = 0.0864 + 0.884K_d(490) - \frac{0.00137}{K_d(490)}$$

Field $E_{d_noon}(6.1 \text{ m}) \pm 2\text{SE}$ for the month of March was $324 \pm 34 \mu\text{mol photons m}^{-2} \text{ s}^{-1}$ (Fig. 1b). The common tank was shaded to approximate in situ field conditions (mean $\pm 2\text{SE}$ tank $E_{d_noon} = 298 \pm 54 \mu\text{mol photons m}^{-2} \text{ s}^{-1}$, Fig. 1b) and prevent photoinhibition that might result from exposure to unshaded irradiances in the tank. Areas of the tank with $E_{d_noon} < 200 \mu\text{mol photons m}^{-2} \text{ s}^{-1}$ were noted and no nubbins were placed in those areas to maintain irradiance levels near in situ values (Fig. 1c). Nubbins were repositioned in the tank each day to randomize any position effects.

Thermal exposure experiments

Two experiments were conducted wherein nubbins were subjected to either an acute or cumulative thermal exposure to determine thermal performance curves of F_v/F_M , R , and P_g . Corals in the acute treatment were moved directly from the ambient to the target temperature (heat shock), while corals in the cumulative treatment experienced gradual (30 min) warming from ambient to subsequent target temperatures (heat accumulation). Average in situ temperatures for the time of year are $> 24 \text{ }^\circ\text{C}$ in late March ($n=7$ years; Fig. 1a, inset), and the observed local bleaching threshold for *A. cervicornis* is $> 31 \text{ }^\circ\text{C}$ (Goergen personal communication). Therefore, experimental temperatures between 25 and 36 $^\circ\text{C}$ were selected to obtain a range of metabolic rates from the baseline for the time of year to those wherein a physiological

decline was expected to capture the upper breadth of thermal performance of *A. cervicornis*. Each exposure was completed within a single day to make the exposures comparable and avoid acclimation. Experiments were carried out over two days between 0900 and 1730 h local time.

Experiments were performed in laboratory aquaria comprised of two tank systems: a staging system and a heat treatment system. Each system consisted of an experimental tank and sump tank constructed from 25-L insulated coolers. Water was pumped to the experimental tank by a 450-W electric pump and returned to the sump tank via gravity overflow (Fig. S1, ESM). Both staging and heat treatment systems were filled with fresh seawater from the outdoor tank each morning. Additional fresh seawater was supplied continuously at a rate of 4 L h⁻¹ into each experimental tank from a common reservoir, and the addition of water to the system was balanced by outflow from the sump tank. The acute and cumulative exposures were performed in the same heat treatment system.

Temperature was controlled by a submersible heater and pump for chilling in the sump, driven by an Arduino microprocessor and custom software. The chilling pump circulated tank water through a stainless-steel coil in an ice bath maintained at 4 °C by a temperature controller (AquaLogic). Tank water temperature was monitored by a thermistor in the experimental tank calibrated to 0.1 °C against a NIST-traceable spirit-filled thermometer and recorded at 1 kHz by the Arduino logger. The temperatures of all laboratory tanks matched the ambient temperature of the outdoor tank (25.4 °C) when corals were brought into the laboratory.

A custom 8-chamber respirometry apparatus was submersed in the experimental tank of the heat treatment system (Fig. S2, ESM). Each 120-mL chamber within the apparatus was fitted with a glass-enclosed magnetic stir bar and a fiber optic oxygen (O₂) sensor connected to a PreSens OXY-10 Mini instrument. All chambers were mounted to an acrylic base over magnetic micro-stirrers. Water temperatures were measured in each chamber to ensure temperature between the saltwater bath and chamber were the same. A two-point calibration was performed on the O₂ sensor in each chamber according to the manufacturer's protocol. O₂ concentrations ([O₂]) were recorded in all chambers every 6 s.

For both exposures, nubbins were transferred from the outdoor tank to the experimental tank of the staging system in the laboratory. One nubbin was placed randomly into each of the temperature-stabilized chambers, with a single chamber left empty to measure microbial metabolism in the seawater. In the acute exposure, one ramet from each genet ($n=6$ genets) was placed directly into one of the chambers. Measurements were made at a single temperature ($n=5$ temperatures), and the nubbins were sacrificed. No nubbin was measured at more than one temperature in the acute exposure and the same six genets were present at each

measurement temperature, with one exception. The mortality of a nubbin from genet F in the field permitted only five genets to be measured at 27.9 °C, resulting in a total of 29 nubbins in the acute exposure.

In the cumulative exposure, as above, seven nubbins (genets B-J) were placed into the chambers at 25.4 °C. The O₂ metabolism of these individuals was measured repeatedly as temperature was incrementally ramped to five temperatures between 25.4 and 35.7 °C. Six of the seven genets were the same as those in the acute experiment. Nubbins from the cumulative exposure were subjected to each measurement temperature for at least 20 min, then ramped up by 2.5 °C in 30-min intervals. This design was chosen for two reasons. First, if different exposures produced the same physiological patterns, a cumulative exposure would substantially reduce the number of coral nubbins required. Second, the rates of temperature increase were selected to complete the temperature exposure series within a single day in both exposures, to avoid confounding the exposure response with possible acclimation.

Response variables

Rates of dark respiration (R) and light-saturated net photosynthesis (P_n) were quantified by measuring O₂ evolution with the coral respirometry apparatus at five distinct measurement temperatures. A single nubbin was placed in each chamber, the chambers were sealed, and [O₂] was measured for > 10 min in the dark. The chambers were opened and flushed with tank water. After at least 25 min in the dark, F_v/F_M was measured in triplicate at different places on each nubbin using a pulse-amplitude modulation fluorometer (Junior-PAM, Heinz Walz GmbH). All chambers were resealed, and the tank was illuminated with a photosynthesis-saturating irradiance of 500 μmol photons m⁻² s⁻¹ via white LED lamps, based on experimental measurements performed by Chalker (1981) and Bedwell-Ivers et al. (2017). Incubation irradiances were verified using a Li-Cor 250A PAR radiometer with a scalar (spherical) collector. Net O₂ flux was measured at each temperature in the light. The entire process was repeated at five distinct temperatures from 25.4 to 35.7 °C, at 2.5–3 °C intervals during each exposure treatment (Fig. 2a). Salinity was measured using a refractometer at every temperature. Differences in O₂ solubility due to temperature and salinity were compensated for in all calculations during data processing.

Data processing and analyses

The ambient temperature of the outdoor tank was 25.4 °C. Degree heating times are often calculated as the duration and magnitude of temperatures > 1 °C above the local mean monthly maximum (Wyatt et al. 2020). However, because we

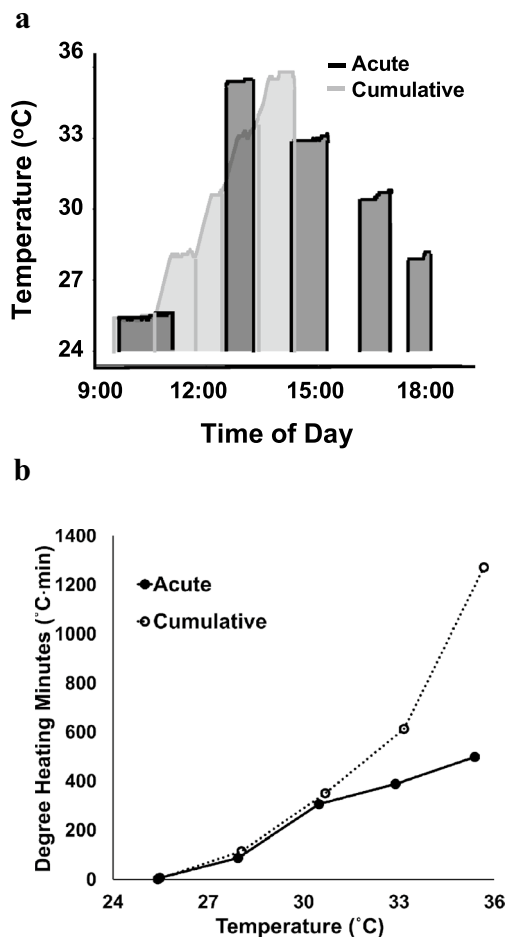


Fig. 2 **a** The temperature series (°C) of two thermal exposures, wherein coral holobiont respiration and net photosynthesis were measured at 5 discrete temperatures (thermal plateaus) for at least 20 min (10 min for dark respiration and 10 min for net photosynthesis). Corals in the acute exposure were placed into the chambers at the target temperature (solid black lines) for the duration (dark grey shading). Corals in the cumulative exposure were placed in chambers at the start of the experiment and ramped up at ~2.5 °C intervals in ~30 min (light gray shading). **b** The thermal dose expressed in degree heating minutes (DHMs, °C·min) above ambient (25.4 °C) for acute (solid points and line) and cumulative (open points, dotted line) exposures, calculated by integrating the shaded areas in Fig. 2a. There was error in both x and y, but the 95% confidence limits on both are smaller than the symbols plotted

were interested in comparing laboratory exposures, thermal dose from the recorded temperature series of each treatment was calculated as degree heating minutes (DHM, °C·min) above the ambient temperature. Briefly, the magnitude of temperatures > 25.4 °C were summed over the total exposure duration (min) for each set of nubbins (Table S1, ESM).

Triplicate measurements of F_V/F_M were averaged and reported as single values (without error) for each nubbin at each measurement temperature. R , P_n , and P_g were calculated from changes in dissolved $[O_2]$ as in Aichelman

et al. (2019). Recorded $[O_2]$ values were corrected for temperature and salinity based on the correction calculations provided by the PreSens system. Slopes of $\Delta O_2/\Delta t$ ($\text{nmol } O_2 \text{ mL}^{-1} \text{ min}^{-1}$) in the dark (R) and in the light (P_n) were calculated from linear sections of each trace by least squares regression. Metabolic rates were corrected for the combined effects of instrument drift and microbial metabolism from the seawater, scaled to chamber volume (mL), and normalized to coral tissue surface area (cm^2 , determined by the wax method, Stimson 1991). Gross photosynthesis (P_g) was calculated as $P_n + |R|$.

Since temperature is a continuous variable, we performed regression analyses, rather than parametric or non-parametric analyses with pairwise comparisons, to determine the functional responses across the entire temperature range and obtain a predictive model for thermal performance (Cottingham et al. 2005). Thermal performance under each exposure was approximated using a modified Sharpe–Schoolfield model (Schoolfield et al. 1981), which extends the classic Arrhenius model for thermal performance by accounting for non-linearity of the performance curve from inactivated proteins at high temperatures (reviewed in Schulte 2015). Sharpe–Schoolfield models have been used to accurately describe temperature sensitivity characteristics in a variety of organisms, such as developmental rates of *Drosophila* (Gibert and Jong 2001), primary productivity of phytoplankton (Padfield et al. 2016), and metabolic adaptation of temperate corals (Aichelman et al. 2019). Values of F_V/F_M , R , and P_g vs. temperature were each fitted to a modified Sharpe–Schoolfield model (Padfield et al. 2016):

$$\ln[m(T)] = E_a \left(\frac{1}{kT_c} - \frac{1}{kT} \right) + \ln[m(T_c)] - \ln \left[1 + e^{\frac{E_h}{k} \left(\frac{1}{T_h} - \frac{1}{T} \right)} \right]$$

using MATLAB's Curve Fitting Tool (cftool), which provided error estimates for each non-linear equation parameter as in Zimmerman et al. (1987). Model symbols and their definitions are summarized in Table 1. The model assumes that a single enzyme controls the apparent temperature dependence of the rate (Padfield et al. 2016). The lower limit of Symbiodiniaceae photosynthesis in culture has been reported to be 5 °C (McBride et al. 2009) and many enzymes and proteins critical to cellular function denature around 40 °C (Angilletta 2009). As such, a metabolic rate of 0 was assumed at 5 and 40 °C for all Sharpe–Schoolfield model fits in both exposures.

Values of F_V/F_M , R , and P_g vs. DHM were each fitted to a 2nd degree polynomial:

$$\ln[m(T)] = a(\text{DHM}^2) + b(\text{DHM}) + c$$

as above, where parameter a is the 2nd order slope, b is the 1st order slope, and c is the y-intercept (Table 1). Resulting parameters for all models were compared via t tests to

Table 1 Symbols, definitions, and units used for model parameters

Symbol	Definition	Units
$m(T)$	Metabolic rate per unit surface area	$\text{nmol O}_2 \text{ cm}^{-2} \text{ min}^{-1}$
E_a	Activation energy for the metabolic process	eV
E_h	Inactivation energy for the metabolic process $> T_h$	eV
$m(T_c)$	Metabolic rate at T_c	$\text{nmol O}_2 \text{ cm}^{-2} \text{ min}^{-1}$
T_c	Reference temperature, 298.55 K (25.5 °C)	K
T_h	Temperature at which enzymatic inactivation begins	K
k	Boltzmann's constant (8.62×10^{-5})	eV K^{-1}
T	Temperature	Kelvin, K
a	2nd order slope	$\text{nmol O}_2 \text{ cm}^{-2} \text{ }^\circ\text{C}^{-1} \text{ min}^{-2}$
b	1st order slope	$\text{nmol O}_2 \text{ cm}^{-2} \text{ }^\circ\text{C}^{-1} \text{ min}^{-2}$
c	y-intercept	$^\circ\text{C}\cdot\text{min}$

identify significant differences in curve features between acute and cumulative exposures ($\alpha = 0.05$, mean \pm 95% confidence interval).

Temperature sensitivity (Q_{10}) was calculated over the exponentially increasing portion of the response curve from 25 to 33 °C for each metabolic rate with acute and cumulative exposures, as follows:

$$Q_{10} = \left(\frac{\rho_2}{\rho_1} \right)^{\left(\frac{10}{T_2 - T_1} \right)}$$

where ρ is the metabolic rate and T is the corresponding temperature. Unlike the Sharpe–Schoolfield model, metabolic rates that decreased at high temperatures were eliminated from these calculations, as the Q_{10} formulation requires that metabolic rates increase continuously throughout the temperature range. The ratio of instantaneous rates of gross photosynthesis to respiration ($P_g:R$) was calculated for each sample, and an analysis of covariance was performed to compare the temperature dependence of $P_g:R$ for each exposure. Raw data are publicly available on GitHub and citable at Zenodo (Martell 2021).

Results

Daily mean temperatures \pm 2SE in the field and outdoor tank over the course of the experiment were 24.4 ± 0.3 and 26.0 ± 0.1 °C, respectively (Fig. 1a). On the morning of both exposures, the outdoor tank temperature was 25.4 °C when corals were transferred to the laboratory (Fig. 2a). At temperatures < 30 °C, DHM ($^\circ\text{C min}$) were similar between exposures (Fig. 2b). At temperatures > 30 °C, nubbins in the cumulative treatment were exposed to two to three times greater DHM than in the acute treatment.

Temperature responses of all metabolic parameters (F_v/F_M , R , P_g) in both the acute and cumulative exposures conformed to the Sharpe–Schoolfield model (Table S2, Fig.

S3, ESM). T_h was the inflection point of the thermal performance curve and indicated the temperature where the enzymatic inactivation (E_h) of the physiological parameter occurred. The T_h of F_v/F_M was 4.9 °C lower in the acute exposure relative to the cumulative exposure (Table 2; Fig. S3A, ESM).

F_v/F_M decreased when temperatures exceeded 28 °C in both treatments, representing a thermal dose > 75 °C·min (Fig. 3a). Mean F_v/F_M dropped by 65% from 0.55 to 0.19 in the acute exposure but decreased by only 21% from 0.58 to 0.46 with cumulative heating (Fig. 3a). In the acute exposure, F_v/F_M decreased linearly as thermal dose increased from 0 to 247 °C·min, then declined sharply at 326 °C·min (Fig. 3a). In contrast, the slope of F_v/F_M vs. thermal dose in the cumulative exposure was less steep and never fell below 0.45, despite being exposed to > 900 °C·min, nearly three times the thermal dose of the acute exposure.

Exposure regime (acute vs. cumulative) had a significant effect on the Sharpe–Schoolfield model parameters for R and P_g (Table 2). The temperature-induced enzyme activation values (E_a) for R in this study ($E_{a \text{ ACUTE}} = 0.76 \pm 0.07$ eV; $E_{a \text{ CUMULATIVE}} = 0.74 \pm 0.05$ eV) were on par with those expected for invertebrates (e.g., $E_{a \text{ INVERT}} \propto \sim 0.60$ to 0.70 eV, Brown et al. 2004). Baseline values of R , $m(T_c)$, and E_a of R were not affected by the thermal exposure regime, but T_h and the energy required for the onset of enzyme inactivation (E_h) were significantly higher in the cumulative exposure than in the acute exposure (Table 2). T_h was 1.5 °C lower in the acute exposure indicating, as with F_v/F_M , that holobiont R was more sensitive to acute thermal challenge than to cumulative exposure.

Every Sharpe–Schoolfield model parameter for P_g differed with exposure primarily because P_g remained higher above 30 °C for the cumulative treatment than the acute treatment. E_a and $m(T_c)$ of P_g were slightly, but significantly, higher in the acute exposure (Table 2). T_h and E_h of P_g were 4.3 °C and 0.53 eV greater in the cumulative exposure, respectively (Table 2). The acute exposure P_g measurements

Table 2 Mean parameters values ($\pm 95\%$ CI) for the effect of temperature on maximum dark-adapted yield of PSII (F_v/F_M), respiration (R), and gross photosynthesis (P_g) in acute and cumulative exposures and the t statistic (t), degrees of freedom (df), and p values (p) from comparisons (t tests) of parameters between exposures

	Parameter	Acute	Cumulative	t	df	p
F_v/F_M	E_a	0.15 ± 0.02	0.16 ± 0.02	1.17	11	0.267
	E_h	3.44 ± 1.30	1.57 ± 0.19	3.79	11	0.003
	$m(T_c)$	1.42 ± 0.04	1.47 ± 0.03	2.57	11	0.026
	T_h	36.6 ± 0.7	41.5 ± 0.2	17.81	11	< 0.0001
R	E_a	0.76 ± 0.07	0.74 ± 0.05	0.60	11	0.561
	E_h	2.67 ± 0.60	4.30 ± 1.04	3.38	11	0.006
	$m(T_c)$	3.15 ± 0.13	3.11 ± 0.08	0.68	11	0.510
	T_h	36.1 ± 1.0	37.6 ± 0.6	3.34	11	0.007
P_g	E_a	1.34 ± 0.19	1.15 ± 0.08	2.42	11	0.034
	E_h	1.40 ± 0.30	1.93 ± 0.24	3.54	11	0.005
	$m(T_c)$	4.84 ± 0.49	4.28 ± 0.17	2.85	11	0.016
	T_h	28.6 ± 2.9	32.9 ± 1.1	3.65	11	0.004

T_h temperatures are given in $^{\circ}\text{C}$

p values representing significant differences between exposures for each parameter are bolded

displayed a high degree of variability and 95% confidence intervals overlapped (Fig. S3C, ESM), but differences in model parameters were significant.

R in the acute exposure peaked at $121^{\circ}\text{C}\cdot\text{min}$ and declined at $\text{DHM} > 121^{\circ}\text{C}\cdot\text{min}$. In the cumulative exposure, however, R continued to increase at $\text{DHM} > 543^{\circ}\text{C}\cdot\text{min}$ and temperatures $> 31^{\circ}\text{C}$ and plateaued at thermal doses $> 1000^{\circ}\text{C}\cdot\text{min}$, despite being exposed to a thermal dose more than eight-fold higher than in the acute treatment (Table 3, Fig. 2b). Rates of P_g in both exposures increased until DHM exceeded $\sim 325^{\circ}\text{C}\cdot\text{min}$ (i.e., from 25 to 31°C), then decreased with increasing DHM (Fig. 2b, c). Mean R was more sensitive to increasing temperature than mean P_g in both exposure treatments; however, Q_{10} values for both metabolic rates between treatments were not significantly different (Table 4).

The decline in gross photosynthesis at temperatures $> 30^{\circ}\text{C}$ and thermal doses $> 325^{\circ}\text{C}\cdot\text{min}$ indicated thermal stress, leading to metabolic deficit (i.e., $P_g:R < 1$) at higher temperatures. Examination of the metabolic budget as a function of temperature revealed $P_g:R$ decreased linearly with increasing temperature at the same interval in both exposures but $P_g:R$ in the acute exposure was significantly lower at all temperatures (Fig. 4a; Table 5a). $P_g:R$ dropped below 1 at 34.9 and 36.2°C in the acute and cumulative exposures, respectively (Fig. 4a), indicating the onset of instantaneous metabolic deficit, and reflecting the differences in metabolic rate T_h between exposures (Fig. 3b, c). $P_g:R$ as a function of DHM revealed a sharper decline with acute exposure compared to the cumulative treatment (Fig. 4b; Table 5b). Acute exposure $P_g:R$ as a function of DHM fell below 1 after experiencing just half the thermal dose (DHM) experienced by corals in the cumulative exposure (Fig. 4b). Although $P_g:R$ declined gradually in the cumulative exposure, it never fell below 1, indicating that

the these corals maintained positive metabolic balance at all experimental temperatures (Fig. 4a). Examination of $P_g:R$ as a function of DHM accentuated exposure differences not denoted by examination of temperature alone (Fig. 4a, b).

Discussion

Despite a smaller thermal dose, the acute exposure elicited a greater physiological response in metabolic and F_v/F_M thermal performance, relative to the cumulative exposure. Physiological symptoms of thermal stress were also most apparent in the acute exposure, adhering to the prevailing thermal acclimation theory that more gradual heating can ameliorate thermal stress (Angilletta 2009). All physiological measures had lower temperatures of inactivation, T_h , and R and P_g had lower enzyme inactivation slopes, E_h , with acute exposure. Modeled R and P_g declined more steeply in the acute exposure than in the cumulative exposure (Fig. S3B, ESM). Holobiont R and P_g were not measured at temperatures greater than 35.7°C ; thus, the critical thermal maximum, where R or $P_g = 0$, may have been greater than the upper constraint of 40°C used in the model. An increase in T_h would lead to a steeper E_h , as was observed in both R and P_g . However, given that the onset of denaturation for many critical proteins is around 40°C (Lepock et al. 1993), a large shift in critical thermal maximum seems unlikely in the context of this experiment, especially since it was conducted over a short duration unlikely to generate an acclimation response.

Holobiont respiration showed greater resilience than photosynthesis at high thermal doses, as in previous work (Silbiger et al. 2019). *In hospite* CO_2 limitation has been suggested in zooxanthellate cnidarians under thermal stress (Rädecker et al. 2017; Cuning et al. 2017), which may

Fig. 3 The effect of acute (solid points) and cumulative (open points) thermal dose (degree heating minutes, °C·min) on **a** maximum dark-adapted yield of photosystem II (F_V/F_M), **b** holobiont respiration (R), and **c** gross photosynthesis (P_g). Solid lines are 2nd degree polynomial fits. Dotted and dashed lines are 95% confidence intervals for the acute and cumulative treatments, respectively

explain the sharper decline in P_g than R in response to high thermal doses (> 325 °C·min) observed here. Although we did not measure ΔpH , assuming an initial pH of 8.1, an alkalinity of $2300 \mu\text{mol L}^{-1}$ seawater and equivalency between $\Delta[\text{DIC}]$ and $\Delta[\text{O}_2]$, CO2SYS-based calculations (Pierrot et al. 2006) indicate that air-saturated CO_2 concentration ($[\text{CO}_2]$) in the seawater may have decreased from $8 \mu\text{mol L}^{-1}$ at ambient (25.4 °C) to $5 \mu\text{mol L}^{-1}$ at temperatures > 31 °C. However, coral holobiont photosynthesis does not appear to be stimulated by increased $[\text{CO}_2]$ (Burriss et al. 1983; Comeau et al. 2017, but see Osinga et al. 2017), and both treatment conditions had sufficient bicarbonate concentrations ($[\text{HCO}_3^-] > 1800 \mu\text{mol L}^{-1}$) and aragonite saturation states ($\Omega_{\text{Ar}} > 4$) to support photosynthesis and calcification, respectively. Thus, CO_2 limitation probably did not contribute to the reduction in P_g observed in this experiment.

F_V/F_M reduction was much less severe in the cumulative exposure than in acutely exposed corals, despite greater DHM at higher temperatures in the cumulative exposure. The drastic reduction of F_V/F_M and significantly reduced T_h of F_V/F_M with increased temperature are consistent with photosystem II (PSII) damage in the alga with acute heat shock (Warner et al. 1999), suggesting algal symbiont PSII was particularly sensitive to the acute exposure. The dramatic decline in F_V/F_M observed with acute heat shock may result in the inability to replace important PSII structural proteins, such as D1, quickly enough under such exposure regimes, leading to photosystem breakdown (Warner et al. 1999).

The thermal performance of *A. cervicornis* was less detrimentally affected by high temperatures with slower, incremental heating that acute heat shock, and respiration was less affected than photosynthesis. Thermal peaks of metabolic performance curves were shifted to higher temperatures with cumulative exposure (Fig. S3, ESM), supporting the idea that lower heating rates enabled detectable physiological adjustment (Middlebrook et al. 2010), even over the very short time periods used here. Acute treatment corals were exposed to instantaneous heating rates when transferred directly from 25.4 °C to each measurement temperature, while cumulative treatment corals were heated at a rate of 2 °C h^{-1} between each temperature increase. While neither heating rate is representative of local field conditions, these exposure regimes generated significant physiological differences that underscore the importance of heating rate in coral physiology. Despite its importance, fewer than

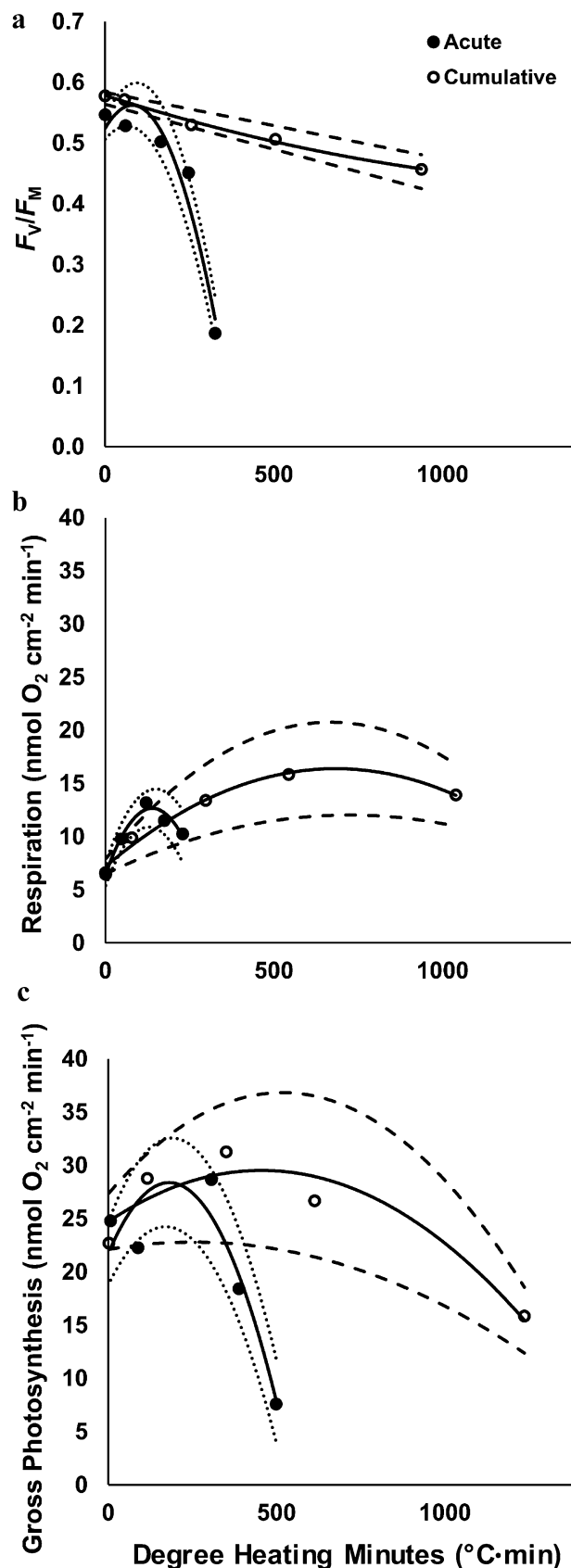


Table 3 Mean 2nd degree polynomial parameter values ($\pm 95\%$ CI) for the effect of degree heating minutes on maximum dark-adapted yield of PSII (F_V/F_M), respiration (R), and gross photosynthesis (P_g) in acute and cumulative exposures and the t statistic (t), degrees of freedom (df), and p values (p) from comparisons (t tests) of parameters between exposures

	Parameter	Acute	Cumulative	t	df	p
F_V/F_M	a	$-3.13E-06 \pm 4.80E-07$	$4.57E-08 \pm 2.17E-08$	7.19	11	0.0001
	b	$9.44E-04 \pm 2.42E-04$	$1.49E-04 \pm 2.86E-05$	4.87	11	0.0005
	c	0.52 ± 0.02	0.58 ± 0.01	2.93	11	0.01
R	a	$-7.10E-05 \pm 1.87E-05$	$-1.74E-05 \pm 4.51E-06$	3.00	11	0.01
	b	0.04 ± 0.01	0.03 ± 0.01	1.61	11	0.14
	c	6.32 ± 0.90	6.90 ± 1.09	0.40	11	0.69
P_g	a	$-2.11E-04 \pm 4.56E-05$	$-2.15E-05 \pm 7.01E-06$	4.45	11	0.001
	b	0.08 ± 0.02	0.02 ± 0.01	2.36	11	0.04
	c	22.41 ± 2.19	24.57 ± 2.09	0.71	11	0.49

p values representing significant differences between exposures for each parameter are bolded

Table 4 The mean Q_{10} ($\pm 95\%$ CI) of each metabolic rate calculated from 25 to 31 °C for acute respiration and both exposures of gross photosynthesis

Metabolic rate	Q_{10}		t	df	p
	Acute	Cumulative			
R	4.37 ± 1.94	3.57 ± 1.87	0.592	11	0.57
P_g	1.38 ± 0.40	2.10 ± 0.94	1.320	11	0.21

Q_{10} of respiration in the cumulative exposure was calculated from 25 to 33 °C

The t statistic (t), degrees of freedom (df), and p values (p) from Q_{10} comparisons (t tests) of respiration (R) and gross photosynthesis (P_g) rates between exposures

20% of coral thermal stress studies reported heating rates (McLachlan et al. 2020). The influence of heating rates on coral physiology warrants further investigation.

Differences in metabolic rates and $P_g:R$ between treatments were more pronounced as a function of degree heating minutes (Figs. 3, 4b) than temperature (Figs. S3, 4a). Examination of metabolic rates as a function of DHM revealed P_g to be more dramatically reduced at high DHM than R (Fig. 3), indicating symbiont stress. These observations were noticed only by expressing the exposures as DHM, demonstrating the value in using a dose-context for thermal stress experiments. By placing temperature exposures in degree heating times, subtle physiological differences may be more easily identified. In addition, short-term temperature exposures are typical in laboratory experiments for logistical reasons (McLachlan et al. 2020), but there is often a disconnect between laboratory-based exposures and thermal regimes on the reef. Calculation of thermal doses allows exposures in the laboratory to be related to the field, providing a common currency for interspecific and cross-study comparisons. The use of degree heating times also enables the conversion of temperature exposures into energy (i.e., Joules), which can allow metabolic budgets to be determined and generalizations to be made over larger scales.

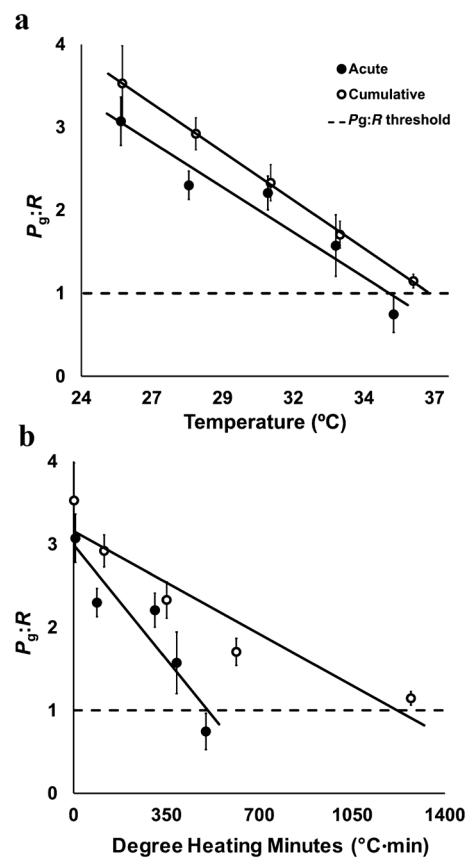


Fig. 4 The mean ratio of gross photosynthesis to respiration ($P_g:R$) as a function of temperature **a** and thermal stress dose expressed as degree heating minutes **b** in acute (solid points) and cumulative (open points) exposures. Error bars are 95% confidence intervals. Dashed line indicates a metabolic deficit threshold where $P_g:R < 1$

The obligate nature of many scleractinian symbioses underscores the reliance upon the metabolic energy derived from algal symbiont photosynthesis for holobiont survival and growth. Assuming a sinusoidal function for daylength at the nursery latitude, and calculating the hours

Table 5 The analysis of covariance results from the $P_g:R$ as a function of temperature (a) and degree heating minutes (b)

(a)						
$P_g:R$ vs. Temperature	<i>df</i>	Sum sq	Mean sq	<i>F</i>	<i>p</i>	
Treatment	1	1.94	1.94	18.33	7.34E-05	
Temperature	1	38.01	38.01	359.94	4.70E-26	
Treatment × Temperature	1	0.03	0.03	0.31	0.58	
Error	56	5.91	0.11			
(b)						
$P_g:R$ vs. DHM	<i>df</i>	Sum sq	Mean sq	<i>F</i>	<i>p</i>	
Treatment	1	8.91	8.91	51.45	1.79E-09	
DHM	1	30.43	30.43	175.76	6.48E-19	
Treatment × DHM	1	3.82	3.82	22.07	1.75E-05	
Error	56	9.70	0.17			

The degrees of freedom (*df*), sum of squares (Sum Sq), mean square (Mean Sq), *F*-statistic (*F*), and *p* value (*p*) are presented. Significant *p* values are bolded.

of saturating irradiance at depth from daily PAR, instantaneous $P_g:R$ can be scaled to daily rates of $P_g:R$ (Zimmerman et al. 1994). On a day with the maximum $E_{d_noon}(z)$ at the coral nursery's latitude, 12 h of saturating irradiance leads to $P_g:R < 1$ at temperatures ≥ 31 °C, corresponding to the local bleaching threshold (NOAA Coral Reef Watch 2017). Metabolic deficits degrade coral health (Levas et al. 2016); however, little is known about how long a deficit must persist to see visual manifestation of dysbiosis (i.e., coral bleaching). Novel conservation interventions, such as marine cloud brightening and reef-cooling (National Academies of Sciences, Engineering, and Medicine 2018), are more likely to be successful if undertaken before bleaching occurs. Future work should be aimed at continuous monitoring of the thermally dynamic metabolic budget relationship (i.e., $P_g:R$), as it may offer a mechanism to identify times of greatest bleaching vulnerability, prioritize restoration target regions, and improve coral bleaching prediction.

Supplementary Information The online version contains supplementary material available at <https://doi.org/10.1007/s00227-021-03847-6>.

Acknowledgements We are grateful to E. Goergen, D. Gilliam, NSU CRRAM Lab, D. Kerstetter, D. Renegar, N. Turner, R. Martell, B. Riegl, H. Nylander-Asplin, V. Pecci, A. Peterson, S. Eagan, D. Swack, and D. Barshis for laboratory and field resources. H. Gaff, D. Gautier, M. Warner, and S. Donner provided guidance on the experimental design and comments on early versions of the manuscript. We thank three anonymous reviewers for their generous comments and suggestions that greatly improved the manuscript. This work was performed

in partial fulfillment of the requirements for the Ph.D. degree (HAM) in Biological Sciences at Old Dominion University.

Author contributions HAM and RCZ conceived the manuscript, analyzed the data, and wrote the paper. HAM led and performed all field and lab work.

Funding This research was supported by Old Dominion University via start-up funds to D. Barshis, a research award from ODU's Biology Graduate Student Organization to HAM and more than 100 anonymous donations made to HAM via a crowdfunding campaign entitled "Training Corals to Resist Bleaching".

Data availability Data are publicly available from on Github at https://github.com/harmonymartell/Acervicornis_physiology_2017.git and citable at Zenodo <https://zenodo.org/badge/latestdoi/233725958>.

Declarations

Conflict of interest The authors declare no conflicts of interest.

Ethical approval Coral samples and data were collected under Florida FWCC Special Activity License # SAL-17-1866-SRP.

Informed consent for publication All authors consent to publication.

References

- Aichelman HE, Zimmerman RC, Barshis DJ (2019) Adaptive signatures in thermal performance of the temperate coral *Astrangia poculata* (Ellis & Solander, 1786). *J Exp Biol* 5:222. <https://doi.org/10.1242/jeb.189225>

- Angilletta MJ (2009) Thermal adaptation: a theoretical and empirical synthesis. Oxford University Press. <https://doi.org/10.1093/acprof:oso/9780198570875.001.1>
- Baums IB, Johnson ME, Devlin-Durante MK, Miller MW (2010) Host population genetic structure and zooxanthellae diversity of two reef-building coral species along the Florida Reef Tract and wider Caribbean. *Coral Reefs* 29:835–842. <https://doi.org/10.1007/s00338-010-0645-y>
- Bedwell-Ivers HE, Koch MS, Peach KE, Joles L, Dutra E, Manfrino C (2017) The role of *in hospite* zooxanthellae photophysiology and reef chemistry on elevated pCO₂ effects in two branching Caribbean corals: *Acropora cervicornis* and *Porites divaricata*. *ICES J Mar Sci* 74:1103–1112. <https://doi.org/10.1093/icesjms/fsw026>
- Bosch TCG, Miller DJ (2016) The holobiont imperative: perspectives from early emerging animals. Springer, Vienna, Austria. <https://doi.org/10.1007/978-3-7091-1896-2>
- Brown BE (1997) Coral bleaching: causes and consequences. *Coral Reefs* 16:S129–S138. <https://doi.org/10.1007/s003380050249>
- Brown JH, Gillooly JF, Allen AP, Savage VM, West GB (2004) Toward a metabolic theory of ecology. *Ecology* 85:1771–1789. <https://doi.org/10.1890/03-9000>
- Burriesci MS, Raab TK, Pringle JR (2012) Evidence that glucose is the major transferred metabolite in dinoflagellate-cnidarian symbiosis. *J Exp Biol* 215:3467–3477. <https://doi.org/10.1242/Jeb.070946>
- Burris JE, Porter JW, Laing WA (1983) Effects of carbon dioxide concentration on coral photosynthesis. *Mar Biol* 75:113–116. <https://doi.org/10.1007/BF00405992>
- Chalker BE (1981) Simulating light-saturation curves for photosynthesis and calcification by reef-building corals. *Mar Biol* 63:135–141. <https://doi.org/10.1007/BF00406821>
- Chen H-K, Song S-N, Wang L-H, Mayfield AB, Chen Y-J, Chen W-NU, Chen C-S (2015) A compartmental comparison of major lipid species in a coral-*Symbiodinium* endosymbiosis: evidence that the coral host regulates lipogenesis of its cytosolic lipid bodies. *PLoS ONE* 10:e0132519. <https://doi.org/10.1371/journal.pone.0132519>
- Coles SL, Jokiel PL (1977) Effects of temperature on photosynthesis and respiration in hermatypic corals. *Mar Biol* 43:209–216. <https://doi.org/10.1007/Bf00402313>
- Comeau S, Carpenter RC, Edmunds PJ (2017) Effects of pCO₂ on photosynthesis and respiration of tropical scleractinian corals and calcified algae. *ICES J Mar Sci* 74:1092–1102. <https://doi.org/10.1093/icesjms/fsv267>
- Cottingham KL, Lennon JT, Brown BL (2005) Knowing when to draw the line: designing more informative ecological experiments. *Front Ecol Environ* 3:145–152. <https://doi.org/10.2307/3868542>
- Cunning R, Muller EB, Gates RD, Nisbet RM (2017) A dynamic bioenergetic model for coral-*Symbiodinium* symbioses and coral bleaching as an alternate stable state. *J Theor Biol* 431:49–62. <https://doi.org/10.1016/j.jtbi.2017.08.003>
- Davies PS (1991) Effect of daylight variations on the energy budgets of shallow-water corals. *Mar Biol* 108:137–144. <https://doi.org/10.1007/BF01313481>
- Davy SK, Allemand D, Weis VM (2012) Cell biology of cnidarian-dinoflagellate symbiosis. *Microbiol Mol Biol Rev* 76:229–261. <https://doi.org/10.1128/Mmbr.05014-11>
- Falkowski PG (1984) Light and the bioenergetics of a symbiotic coral. *Bioscience* 34:705–709. <https://doi.org/10.2307/1309663>
- Fitt WK, Warner ME (1995) Bleaching patterns of four species of Caribbean reef corals. *Biol Bull* 189:298–307. <https://doi.org/10.2307/1542147>
- Gates RD, Baghdasarian G, Muscatine L (1992) Temperature stress causes host cell detachment in symbiotic cnidarians: implications for coral bleaching. *Biol Bull* 182:324–332. <https://doi.org/10.2307/1542252>
- Gibert P, Jong GD (2001) Temperature dependence of development rate and adult size in *Drosophila* species: biophysical parameters. *J Evol Biol* 14:267–276. <https://doi.org/10.1046/j.1420-9101.2001.00272.x>
- Gleeson MW, Strong AE (1995) Applying MCSST to coral reef bleaching. *Advances in Space Research* 16:151–154. [https://doi.org/10.1016/0273-1177\(95\)00396-V](https://doi.org/10.1016/0273-1177(95)00396-V)
- Goergen EA, Gilliam DS (2018) Outplanting technique, host genotype, and site affect the initial success of outplanted *Acropora cervicornis*. *PeerJ* 6:e4433. <https://doi.org/10.7717/peerj.4433>
- Grottoli AG, Rodrigues LJ, Parady JE (2006) Heterotrophic plasticity and resilience in bleached corals. *Nature* 440:1186–1189. <https://doi.org/10.1038/nature04565>
- Hoegh-Guldberg O, Poloczanska ES, Skirving W, Dove S (2017) Coral reef ecosystems under climate change and ocean acidification. *Front Mar Sci* 4:158. <https://doi.org/10.3389/fmars.2017.00158>
- Hughes TP, Baird AH, Bellwood DR, Connolly SR, Folke C, Grosberg R, Hoegh-Guldberg O, Jackson JBC, Kleypas J, Lough JM, Marshall P, Nystrom M, Palumbi SR, Pandolfi JM, Rosen B, Roughgarden J (2003) Climate change, human impacts, and the resilience of coral reefs. *Science* 301:929–933. <https://doi.org/10.1126/science.1085046>
- LaJeunesse TC, Parkinson JE, Gabrielson PW, Jeong HJ, Reimer JD, Voolstra CR, Santos SR (2018) Systematic revision of Symbiodiniaceae highlights the antiquity and diversity of coral endosymbionts. *Curr Biol* 28:2570–2580.e6. <https://doi.org/10.1016/j.cub.2018.07.008>
- Lepock J, Frey H, Ritchie K (1993) Protein denaturation in intact hepatocytes and isolated cellular organelles during heat shock. *J Cell Biol* 122:1267–1276. <https://doi.org/10.1083/jcb.122.6.1267>
- Lesser MP (2006) Oxidative stress in marine environments: biochemistry and physiological ecology. *Annu Rev Physiol* 68:253–278. <https://doi.org/10.1146/annurev.physiol.68.040104.110001>
- Lesser MP, Farrell JH (2004) Exposure to solar radiation increases damage to both host tissues and algal symbionts of corals during thermal stress. *Coral Reefs* 23:367–377. <https://doi.org/10.1007/s00338-004-0392-z>
- Levas S, Grottoli AG, Schoepf V, Aschaffenburg M, Baumann J, Bauer JE, Warner ME (2016) Can heterotrophic uptake of dissolved organic carbon and zooplankton mitigate carbon budget deficits in annually bleached corals? *Coral Reefs* 35:495–506. <https://doi.org/10.1007/s00338-015-1390-z>
- Liu G, Eakin CM, Chen M, Kumar A, De La Cour JL, Heron SF, Geiger EF, Skirving WJ, Tirak KV, Strong AE (2018) Predicting heat stress to inform reef management: NOAA coral reef watch's 4-month coral bleaching outlook. *Front Mar Sci* 5:57. <https://doi.org/10.3389/fmars.2018.00057>
- Martell HA (2021) harmonymartell/Acervicornis_physiology_2017: Martell and Zimmerman 2021 (Version 2021-01-25). Zenodo. <https://doi.org/10.5281/zenodo.4465173>
- McBride BB, Muller-Parker G, Jakobsen HH (2009) Low thermal limit of growth rate of *Symbiodinium californium* (Dinophyta) in culture may restrict the symbiont to southern populations of its host anemones (*Anthopleura* Spp.; Anthozoa, Cnidaria)1. *J Phycol* 45:855–863. <https://doi.org/10.1111/j.1529-8817.2009.00716.x>
- McLachlan RH, Price JT, Solomon SL, Grottoli AG (2020) Thirty years of coral heat-stress experiments: a review of methods. *Coral Reefs* 39:885–902. <https://doi.org/10.1007/s00338-020-01931-9>
- Middlebrook R, Anthony KRN, Hoegh-Guldberg O, Dove S (2010) Heating rate and symbiont productivity are key factors determining thermal stress in the reef-building coral *Acropora formosa*. *J Exp Biol* 213:1026–1034. <https://doi.org/10.1242/jeb.031633>
- Mobley C (1994) Light and water: radiative transfer in natural waters. Academic Press, New York
- Morel A, Huot Y, Gentili B, Werdell P, Hooker S, Franz B (2007) Examining the consistency of products derived from various

- ocean color sensors in open ocean (Case 1) waters in the perspective of a multi-sensor approach. *Remote Sens Env* 111:69–88. <https://doi.org/10.1016/j.rse.2007.03.012>
- Morris LA, Voolstra CR, Quigley KM, Bourne DG, Bay LK (2019) Nutrient availability and metabolism affect the stability of coral–Symbiodiniaceae symbioses. *Trends Microbiol* 27:678–689. <https://doi.org/10.1016/j.tim.2019.03.004>
- Muscantine L, Cernichiari E (1969) Assimilation of photosynthetic products of zooxanthellae by a reef coral. *Biol Bull* 137:506–523. <https://doi.org/10.2307/1540172>
- Muscantine L, McCloskey LR, Marian RE (1981) Estimating the daily contribution of carbon from zooxanthellae to coral animal respiration. *Limnol Oceanogr* 26:601–611
- National Academies of Sciences, Engineering, and Medicine (2018) A research review of interventions to increase the persistence and resilience of coral reefs. The National Academies Press, Washington, DC. <https://doi.org/https://doi.org/10.17226/25279>
- NOAA Coral Reef Watch (2017) NOAA Coral Reef Watch version 3.0 daily global 5-km satellite virtual station time series data for southeast Florida, 12 Mar 2013 to 11 Mar 2014
- Osinga R, Derksen-Hooijberg M, Wijgerde T, Verreth JAJ (2017) Interactive effects of oxygen, carbon dioxide and flow on photosynthesis and respiration in the scleractinian coral *Galaxea fascicularis*. *J Exp Biol* 220:2236–2242. <https://doi.org/10.1242/jeb.140509>
- Padfield D, Yvon-Durocher G, Buckling A, Jennings S, Yvon-Durocher G (2016) Rapid evolution of metabolic traits explains thermal adaptation in phytoplankton. *Ecol Lett* 19:133–142. <https://doi.org/10.1111/ele.12545>
- Pierrot D, Lewis E, Wallace DWR (2006) MS Excel program developed for CO₂ system calculations. In ORNL/CDIAC-105a. Carbon Dioxide Information Analysis Center, Oak Ridge National Laboratory, US Department of Energy, Oak Ridge, Tennessee (Vol. 3)
- Rädecker N, Pogoreutz C, Wild C, Voolstra CR (2017) Stimulated respiration and net photosynthesis in *Cassiopeia* sp. during glucose enrichment suggests *inhospite* CO₂ limitation of algal endosymbionts. *Front Mar Sci* 4:267. <https://doi.org/10.3389/fmars.2017.00267>
- Roth MS (2014) The engine of the reef: photobiology of the coral–algal symbiosis. *Front Microbiol* 5:422. <https://doi.org/10.3389/fmicb.2014.00422>
- Schoolfield RM, Sharpe PJH, Magnuson CE (1981) Non-linear regression of biological temperature-dependent rate models based on absolute reaction-rate theory. *J Theor Biol* 88:719–731. [https://doi.org/10.1016/0022-5193\(81\)90246-0](https://doi.org/10.1016/0022-5193(81)90246-0)
- Schopmeyer SA, Lirman D, Bartels E, Gilliam DS, Goergen EA, Griffin SP, Johnson ME, Lusic C, Maxwell K, Walter CS (2017) Regional restoration benchmarks for *Acropora cervicornis*. *Coral Reefs* 36:1047–1057. <https://doi.org/10.1007/s00338-017-1596-3>
- Schulte PM (2015) The effects of temperature on aerobic metabolism: towards a mechanistic understanding of the responses of ectotherms to a changing environment. *J Exp Biol* 218:1856–1866. <https://doi.org/10.1242/jeb.118851>
- Silbiger NJ, Goodbody-Gringley G, Bruno JF, Putnam HM (2019) Comparative thermal performance of the reef-building coral *Orbicella franksi* at its latitudinal range limits. *Mar Biol* 166:126. <https://doi.org/10.1007/s00227-019-3573-6>
- Stimson J (1991) The temporal pattern and rate of release of zooxanthellae from the reef coral *Pocillopora damicornis* under nitrogen-enrichment and control conditions. *J Exp Mar Biol Ecol* 153:63–74. [https://doi.org/10.1016/S0022-0981\(05\)80006-1](https://doi.org/10.1016/S0022-0981(05)80006-1)
- Wang JT, Douglas AE (1999) Essential amino acid synthesis and nitrogen recycling in an alga–invertebrate symbiosis. *Mar Biol* 135:219–222. <https://doi.org/10.1007/s002270050619>
- Warner ME, Fitt WK, Schmidt GW (1999) Damage to Photosystem II in symbiotic dinoflagellates: a determinant of coral bleaching. *Proc Natl Acad Sci* 96:8007–8012. <https://doi.org/10.1073/pnas.96.14.8007>
- Weis VM (2008) Cellular mechanisms of cnidarian bleaching: stress causes the collapse of symbiosis. *J Exp Biol* 211:3059–3066. <https://doi.org/10.1242/jeb.009597>
- Wyatt ASJ, Leichter JJ, Toth LT, Miyajima T, Aronson RB, Nagata T (2020) Heat accumulation on coral reefs mitigated by internal waves. *Nat Geosci* 13:28–34. <https://doi.org/10.1038/s41561-019-0486-4>
- Zimmerman RC, SooHoo JB, Kremer JN, D’Argenio DZ (1987) Evaluation of variance approximation techniques for non-linear photosynthesis—irradiance models. *Mar Biol* 95:209–215. <https://doi.org/10.1007/BF00409007>
- Zimmerman R, Cabello-Pasini A, Alberte R (1994) Modeling daily production of aquatic macrophytes from irradiance measurements: a comparative analysis. *Mar Ecol Prog Ser* 114:185–196. <https://doi.org/10.3354/meps114185>

Publisher’s Note Springer Nature remains neutral with regard to jurisdictional claims in published maps and institutional affiliations.